AD-A078 455 MARYLAND UNIV COLLEGE PARK INST FOR FLUID DYNAMICS --ETC F/G 7/4
INTERACTIONS OF IONS AND ELECTRONS WITH MOLECULES.(U)
MAR 74 M A COPLAN , B SISKIND N00014-67-A-0239-0023

UNCLASSIFIED NL

1 OF 1
AD-
A 078455

END
DATE
FILMED
1-80
DDC

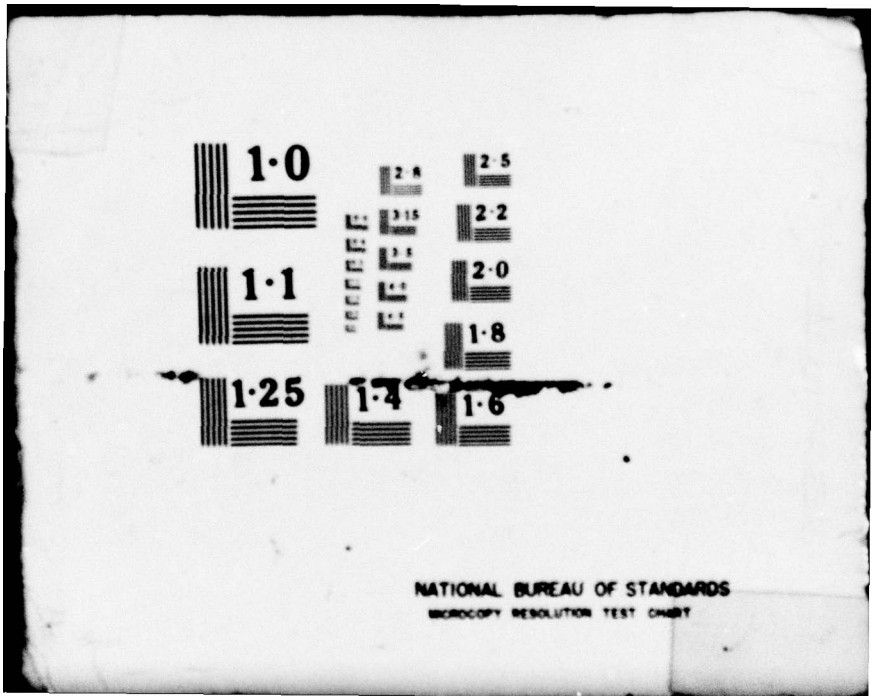
1·0
1·1
1·25
1·4
1·6
1·8
2·0
2·2
2·5
NATIONAL BUREAU OF STANDARDS
MICROCOPY RESOLUTION TEST CHART

INSTITUTE

for

FLUID DYNAMICS

and

APPLIED MATHEMATICS

PROGRESS REPORT

(6) INTERACTIONS OF IONS AND ELECTRONS WITH MOLECULES •

(15) ONR Contract N00014-67-A-0239-0023

(9) Semi-Annual Progress Report 1 July - 31 Dec 73

July 1, 1973 - December 31, 1973

(10) M.A. Coplan and B. Siskind
Institute for Fluid Dynamics and Applied Mathematics
University of Maryland, College Park, Maryland 20742

(11) March 1974 (12) 26

UNIVERSITY OF MARYLAND
College Park

INTERACTIONS OF IONS AND ELECTRONS WITH MOLECULES

ONR Contract N00014-67-A-0239-0023

Semi-Annual Progress Report

July 1, 1973 - December 31, 1973

M. A. Coplan and B. Siskind
Institute for Fluid Dynamics and Applied Mathematics
University of Maryland, College Park, Maryland 20742

March 1974

TABLE OF CONTENTS

I. INTRODUCTION

This report is an account of the progress made in the investigations of rotational and vibrational excitations which occur in collisions of $^6Li^+$ with H_2O molecules in the incident ion energy range from 10 to 40 eV (CM energies of 7.5 to 30 eV for the Li^+ - H_2O system). The large observed inelastic cross sections for the $^6Li^+$ - H_2O system contrast sharply with observations of the scattering of $^6Li^+$ from N_2 in this energy regime where no detectable excitations are found.

The following section is a description of the apparatus used for measuring the angular distributions and energies of the scattered ions. An outline of the progress made on the modifications of the apparatus for use in studies of dissociative excitation by electron impact is also included. In section III the data, current work, and the applications and significance of what has been accomplished are discussed.

II. DESCRIPTION OF EXPERIMENTAL APPARATUS

The apparatus used in these investigations consists of an ion source, gas collision chamber, ion energy analyzer, detector and associated electronics. Except for the electronics, the elements of the experiment are enclosed in a vacuum chamber constructed of aluminum plate rolled into a cylinder 28 inches in diameter and 8 inches high. The chamber is evacuated by a 4 inch diffusion pump to background pressures of 5×10^{-7} torr or better. The ion optics are mounted in aluminum tracks on the underside of the chamber lid which serves as an optical bench. This arrangement is rigid, versatile and provides easy access for adjustments and modifications.

The ion gun assembly, based on a design which has proven quite successful for low-energy charged particle work in the past,[1,2] can rotate ± 30° with respect to the stationary energy analysis section. The ion gun itself consists of stainless steel or (in a later version) copper aperture lenses. The distances between the ion source and the various apertures are maintained with precision sapphire or alumina spheres used as insulating spacers. The entire gun assembly is in turn aligned by means of centerless ground alumina rods in the aluminum tracks fixed to the vacuum chamber lid.

The ion gun uses the multistaging principle[1] in order to maximize current densities. Lithium ions are extracted from the source at a high potential by means of a Soa immersion lens and are then decelerated by a second stage to the energy they will have in the scattering chamber.[2] The ion source[3] is a button of isotopically pure ^{6}Li in the form of an aluminosilicate which when heated by a self-contained tungsten element emits a flux of $^{6}Li^{+}$.

The flexible scattering chamber is a brass bellows with brass cylinders brazed onto either end. One cylinder is held in the ion gun assembly track by the alumina rods and the other is similarly confined in an analogous track preceding the energy analyzer. The cylinders also serve as mounts for the aperture nozzles and the tubes leading to the sample gas source and capacitance manometer used for measuring the pressure of the gas in the scattering chamber. (This pressure is typically in the range 0.5 - 1.0 millitorr for H_2O). The flexibility of the bellows permits rotation of the ion gun assembly with respect to the analyzer and its optics. The aperture nozzles in the scattering chamber define the geometry of the incoming and scattered ion beams, reduce the path length of the ions in

The ion gun assembly, based on a design which has proven quite successful for low-energy charged particle work in the past,[1,2] can rotate ± 30° with respect to the stationary energy analysis section. The ion gun itself consists of stainless steel or (in a later version) copper aperture lenses. The distances between the ion source and the various apertures are maintained with precision sapphire or alumina spheres used as insulating spacers. The entire gun assembly is in turn aligned by means of centerless ground alumina rods in the aluminum tracks fixed to the vacuum chamber lid.

The ion gun uses the multistaging principle[1] in order to maximize current densities. Lithium ions are extracted from the source at a high potential by means of a Soa immersion lens and are then decelerated by a second stage to the energy they will have in the scattering chamber.[2] The ion source[3] is a button of isotopically pure ^{6}Li in the form of an aluminosilicate which when heated by a self-contained tungsten element emits a flux of $^{6}Li^{+}$.

The flexible scattering chamber is a brass bellows with brass cylinders brazed onto either end. One cylinder is held in the ion gun assembly track by the alumina rods and the other is similarly confined in an analogous track preceding the energy analyzer. The cylinders also serve as mounts for the aperture nozzles and the tubes leading to the sample gas source and capacitance manometer used for measuring the pressure of the gas in the scattering chamber. (This pressure is typically in the range 0.5 - 1.0 millitorr for H_2O). The flexibility of the bellows permits rotation of the ion gun assembly with respect to the analyzer and its optics. The aperture nozzles in the scattering chamber define the geometry of the incoming and scattered ion beams, reduce the path length of the ions in

the target gas, and maintain the sample gas pressure in the scattering chamber well above the background pressure in the large vacuum chamber. The rate of sample gas flow into the scattering chamber is controlled by fine metering valves external to the vacuum system. The stability of the ion beam is improved if the inside of the scattering chamber is coated with carbon black from an acetylene flame.[4]

Ions leaving the scattering chamber are focussed by means of a triad of cylinders acting as a pair of so-called "two cylinder lenses."[5] A similar triad follows the analyzer. The cylinder triads, like the ion gun, are held in place in their tracks by alumina rods. In the experiments described below the cylinder triads are operated in the "einzel" mode, i.e., the first and third cylinders are at the same potential, in this case ground potential, and the potential of the center cylinder is set at a focussing voltage.[6] The scattering chamber is also at ground potential and the ion source is held above ground at a potential corresponding to the kinetic energy of the ions entering the scattering chamber.

The electrostatic energy analyzer is of the hemispherical variety[7] and is constructed of gold-plated aluminum. The energy of the ions transmitted by the analyzer is a function of the voltage difference between the hemispheres and their dimensions ; in our case this energy is 0.508 times the voltage across the inner and outer hemisphere. The resolution of the analyzer is characterized by a FWHM of 2%, which at 10 eV incident ion energy is comparable to the thermal energy spread of the incident ions.

The post-analyzer cylinder triad focuses the ions into a Bendix Channeltron continuous dynode electron multiplier.[8] The low background count rate of the Channeltron allows us to measure signal rates of less than 1 $sec.^{-1}$. A shielded emitter follower preamplifier is mounted near the collector of the Channeltron and the output is fed to amplifiers and counting electronics outside the vacuum chamber.

An electrometer measures the ion current intercepted by the apertures of the decelerating portion of the ion gun. This current is used to monitor and correct for changes in the ion current emitted from the thermal source.

The results reported were obtained from the averages of five one-second counting intervals at given laboratory angles and analyzer settings. Background counts with no H_2O in the scattering chamber were taken before and after the measurement of the scattered ion signal with H_2O in the chamber. Evacuation times of 30 minutes were often necessary when H_2O was the scattering gas. In the case of N_2, with evacuation times of seconds, it was feasible to take background counts at each angle and energy setting immediately before or after the N_2-scattered counts. This was also the case with Ne which was used as a reference scattering gas.

The technique of using a monatomic gas with no rotational or vibrational states as a reference scatterer proved to be of considerable utility because of shifts of up to 200 mV which can occur in the ion energy due to "sample gas effects".[9] These effects are well known to practitioners of electron-impact excitation experiments and are probably

caused by absorption of mono and oligolayers of the sample gas on the metallic surfaces. The effect has been reported to be most severe for polar molecules and for H_2O we find shifts of 100-200 mV as opposed to shifts on order of magnitude smaller for N_2.

The energy of the maximum scattered ion intensity at a given scattering angle and incident ion energy was reproducible to within a few tens of millivolts. The normalized scattered ion intensity, i.e., the ion count rate for a given incident ion energy, angle, and analyzer setting divided by the intercepted ion gun current, has been reproducible near the energy scan maxima to within a few percent while the ion optics remain clean. The absolute values of the normalized scattered ion intensities decrease somewhat from run to run because of the gradual deposition of pump-oil decomposition products. A thorough cleaning of the optics restores the measured intensities to their initial values. The relative scattered intensities at the maxima of the energy scans at each angle as well as the relative total scattered intensities (i.e., the ion count summed overall processes) at each angle are reproducible from run to run within a few percent despite the gradual decrease of intensity with time.

Modifications to the apparatus to convert it for use in coincidence experiments combining the time-of-flight measurements of the products of electron-impact dissociative excitation with energy loss measurements on the scattered electrons have been completed. The ion emitter and the bellows scattering can be replaced with a standard indirectly-heated Phillips cathode and a rigid cylindrical interaction chamber, respectively.

The latter contains a series of electrostatic deflection and quenching electrodes along a path at right angles to the electron beam. A second Channeltron can be mounted at the end of this path to detect metastable dissociation products. The signs of the potentials on the charged particle optics can be easily reversed at the power supplier for electron-impact experiments.

III. RESULTS

A preliminary account of our results was presented at the Fifth DEAP Conference, Yale University, 1973. [See Appendix]. This early data for the scattering of $^6Li^+$ from H_2O at an incident ion energy of 10 eV has been supplemented by further work at incident ion energies of 17.5, 25 and 40 eV which like the earlier work demonstrates the dominance of inelastic processes over elastic scattering in the $^6Li^+ - H_2O$ system.

The data (see figures I-IV, for example, which illustrate some of our 10 and 17.5 eV work), exhibit the following general features:

1) At any given incident ion energy the maximum in the scattered ion intensity shifts to lower scattered ion energy with increasing angle of scatter.

2) The difference between the expected energy of the scattered ions assuming elastic scattering and the actual most probable scattered ion energy (i.e., the energy scan maximum) increases as a function of angle.

3) Associated with the shift in energy of the intensity maximum as a function of angle is a broadening of this maximum.

The following conclusions can be drawn regarding the scattering of $^6Li^+$ from H_2O in the CM energy range of 7.5 to 30 eV:

1) The dominant scattering processes for $^6Li^+ - H_2O$ collisions are inelastic with energies in some cases of over a volt going into internal modes of the target molecule.

2) The magnitude of the most probable inelastic energy transfer (as indicated by the intensity maxima in the energy scan at constant laboratory angle) is strongly dependent upon the impact parameter. An ion scattered into a large angle (corresponding to a small impact parameter) is likely to undergo a larger inelastic energy loss than an ion scattered into a small angle (corresponding to a large impact parameter).

3) The lack of any evidence of structure in the energy spectra of the scattered ions indicates that the inelastic transitions are either purely rotational or a mixture of vibrational and rotational. The energy resolution of the apparatus is more than adequate for the resolution of pure vibrational transitions, (the smallest for H_2O being 0.198 eV) but is not sufficient to separate the rotational transitions (which have an average separation of 5 mV in H_2O).

Some comparison data have been obtained for N_2 as the target molecule. These data are qualitatively different from the H_2O data in that there is only a narrow peak in the energy scan of the scattered ions which is unshifted from the elastic scattering energy. We ascribe this difference to the large permanent dipole moment of the H_2O molecule and we note that similar effects have been reported by Giese and coworkers[10] for the low energy scattering of protons from a series of diatomic molecules. There appears to be a correlation between the degree of rotational inelasticity of the ion-molecule collisions process and the magnitude of the permanent dipole moment of the target molecule. Higher order moments and the polariz-

ability of the target molecule and of the projectile ion may also influence the degree of rotational excitation.

For the case of the 10 eV data it is not unreasonable to assume only rotational excitation on the basis of the information available. For example, an energy loss of 800 mV (which occurs at a laboratory angle of about 15°) corresponds to a rotational quantum number, J, of 19 or 20 (using suitably averaged moments of inertia)[11] and can be shown, assuming conservation of angular momentum, to correspond to a reasonable value of the impact parameter, 2.8 Å. Also, the time of passage of a 10 eV $^{6}Li^{+}$ ion across a distance of atomic or molecular dimensions, say 2Å, is of the order of one rotational period ($\sim 10^{-14}$ sec) thus recalling the well-known Massey criterion for collisional excitation.[12]

From our results it can be seen that ionic bombardment of a gas consisting of a mixture of polar and nonpolar molecules can produce selective rotational excitation of the polar molecule and a concomitant nonequilibrium temperature distribution. Since chemical reaction-rate coefficients often depend strongly on the relative populations of the states of the reactant molecules, selective excitation of gas mixtures can be a significant factor in the overall composition and energy balance of the upper atmosphere under nonequilibrium conditions.

IV. Figure Captions

Figure I. 10 eV $^{6}Li^{+}$ + H_2O. Scattered ion intensity as a function of ion energy, in eV, for different laboratory scattering angles. (a = 6.6°, b = 7.6°, c = 8.6°, d = 9.6°, e = 10.6°, f = 11.6°, g = 12.6°, h = 13.6°, i = 14.6°, j = 15.6°). The energies corresponding to elastic scattering are indicated with an arrow for each scattering angle.

Figure II. 17.5 eV $^{6}Li^{+}$ + H_2O. Scattered ion intensity as a function of ion energy, in eV, for different laboratory scattering angles. (a = 7.2°, b = 8.2°, c = 9.2°, d = 10.2°, e = 11.2°, f = 12.2°, g = 13.2°, h = 14.2°, i = 15.7°, j = 17.2°, k = 19.2°). The energies corresponding to elastic scattering are indicated with an arrow for each scattering angle.

Figure III. 10 eV $^{6}Li^{+}$ + H_2O. Relative differential cross section summed over all processes as a function of laboratory scattering angle.

Figure IV. 17.5 eV $^{6}Li^{+}$ + H_2O. Relative differential cross section summed over all processes as a function of laboratory scattering angle.

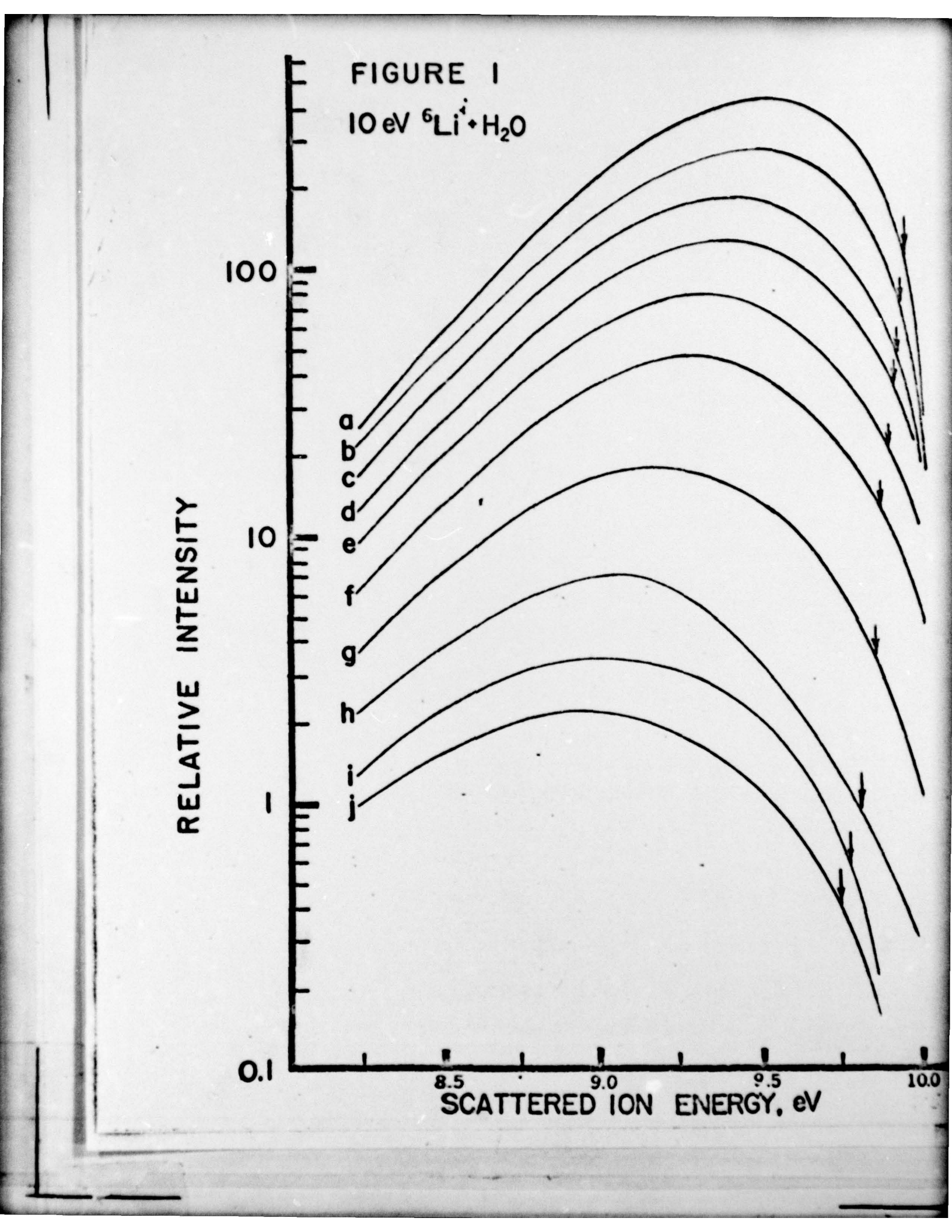
FIGURE 1
10 eV $^6Li^+ + H_2O$
RELATIVE INTENSITY
100
10
1
0.1
a
b
c
d
e
f
g
h
i
j
8.5
9.0
9.5
10.0
SCATTERED ION ENERGY, eV

FIGURE 11

17.5 eV $^{6}Li^{+} + H_2O$

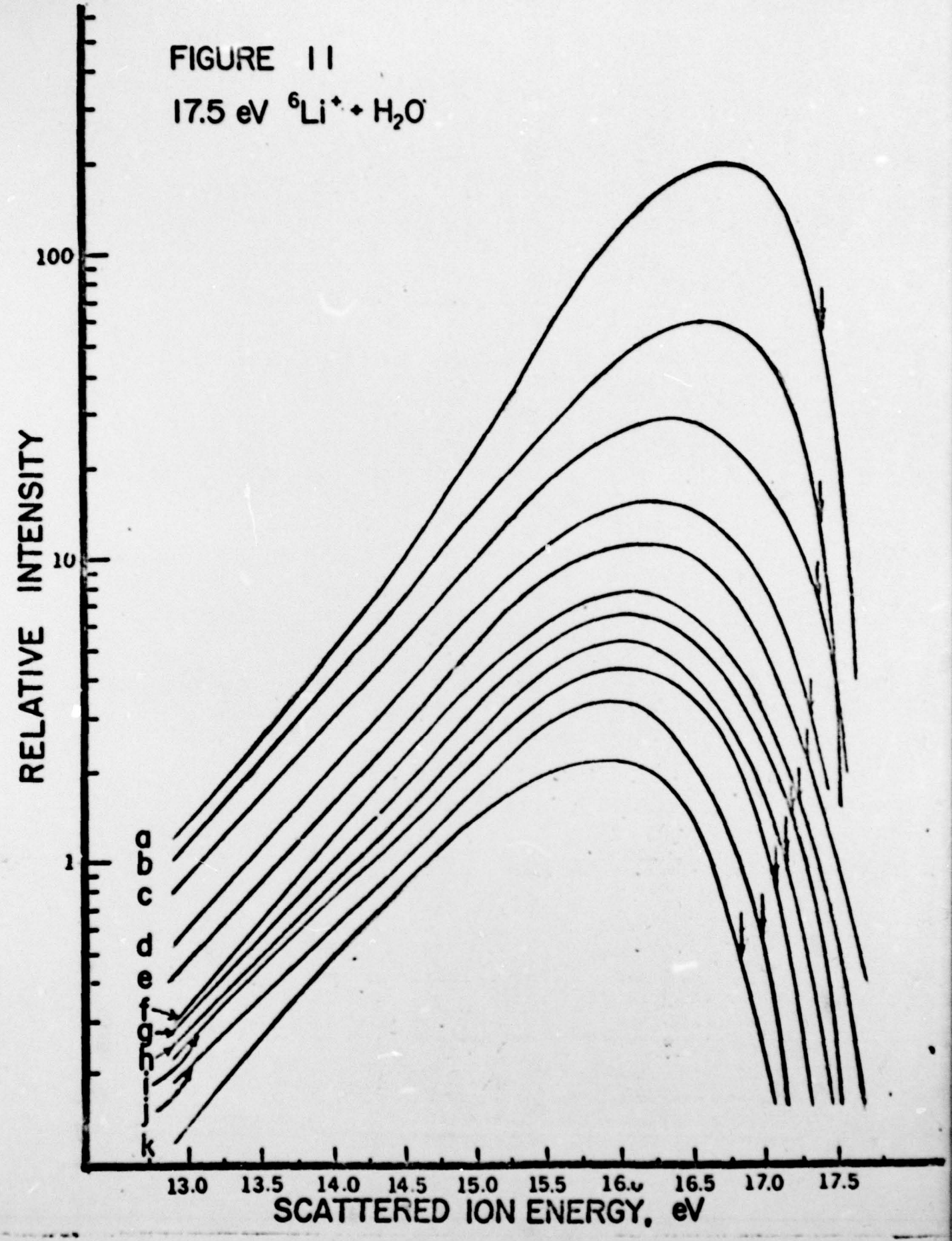

FIGURE 111

10 eV $^{6}Li^{+} + H_2O$

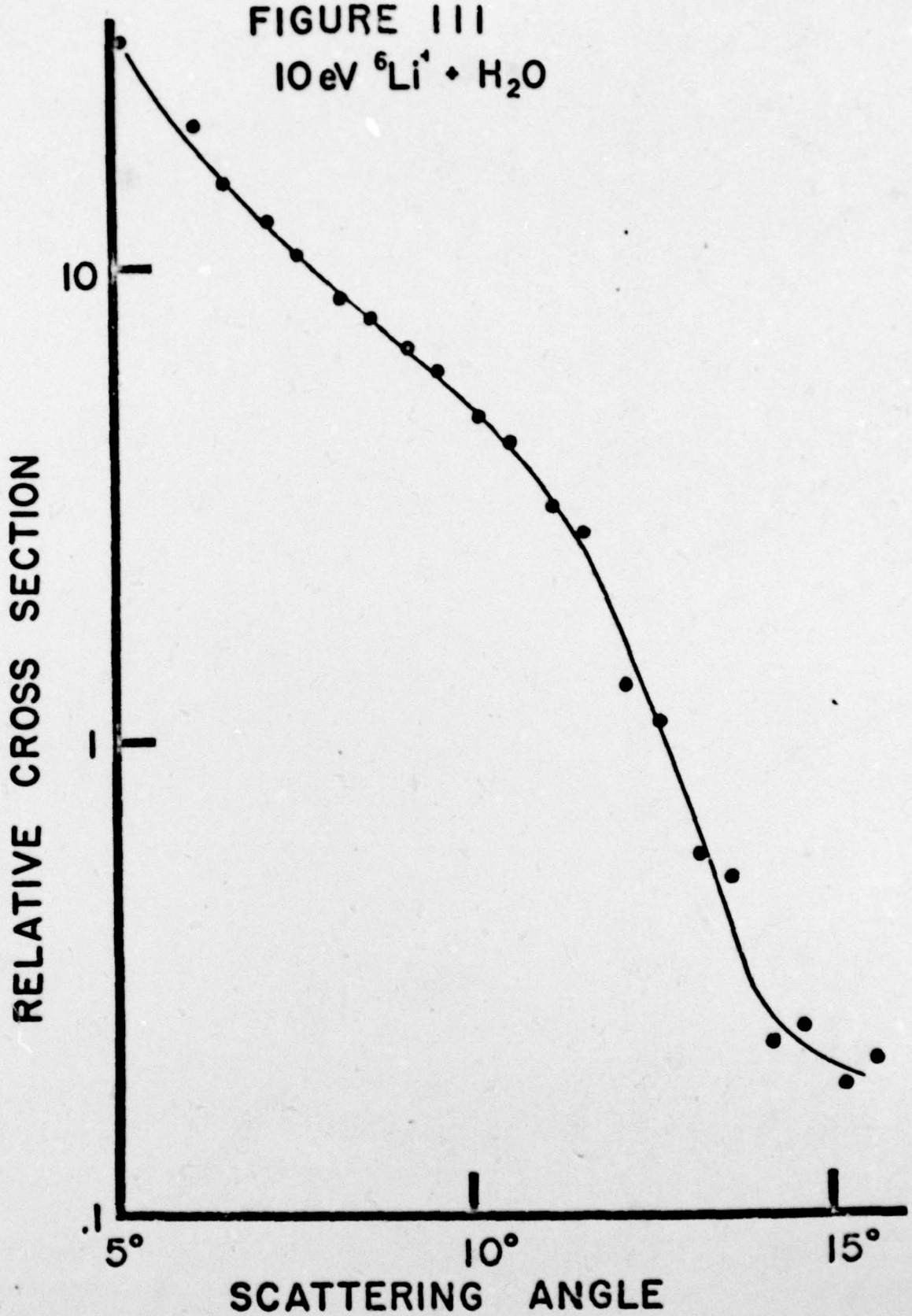

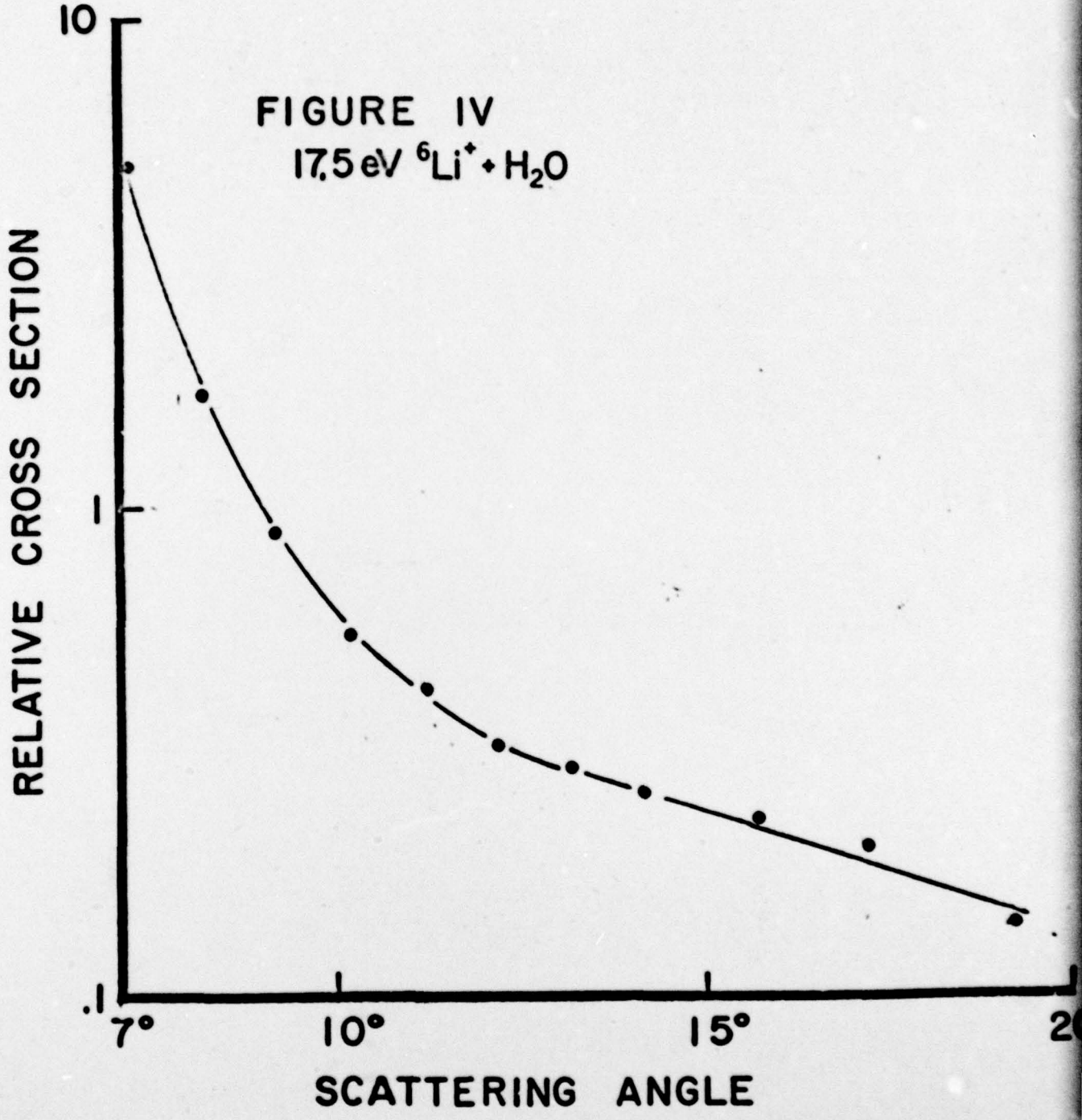

FIGURE IV
17.5 eV $^{6}Li^{+} + H_2O$

V. REFERENCES

1. J. A. Simpson and C. E. Kuyatt, Rev. Sci. Instr. 34, 265 (1963).

2. H. B. Haskell, O. Heinz, and D. C. Lorents, Rev. Sci. Instr. 37, 607 (1966).

3. P. Heinz and R. T. Reaves, Rev. Sci. Instr., 39, 1229 (1968).

4. J. W. McConkey, private communication.

5. K. R. Spangenberg, Vacuum Tubes, McGraw-Hill, New York, 1948, Chapter 13.

6. D.W.O. Heddle, J. Phys. E2, 1046 (1969); D.W.O. Heddle and M.V. Kurepa, J. Phys. E3, 952 (1970).

7. C.E. Kuyatt and J.A. Simpson, Rev. Sci. Instr. 38, 103 (1967).

8. K.C. Schmidt, Bendix Tech. App. Note 9803 (1969).

9. M. Misakian, private communication.

10. H. Udseth, C.F. Giese, and W.R. Gentry, in Proceedings of the Eighth International Conference on the Physics of Electronic and Atomic Collisions, Belgrade, 1973, edited by B.C. Čobić, and M.V. Kurepa (Institute of Physics, Beograd , 1973), p. 93.

11. G. Herzberg, Infrared and Raman Spectra, D. Van Nostrand Co., Princeton, 1945, p. 49, eq. I, 72.

12. N.F. Mott and H.S.W. Massey, The Theory of Atomic Collisions, 3rd Edition, Oxford, 1965, p. 685.

VI. APPENDIX. Report of Initial Results at the Fifth DEAP Meeting, Yale University, New Haven, Conn. December, 1973.

Our present work began as a study of the low-energy elastic scattering of Li^+ ions from water molecules. The affinity of alkali-metal ions for water molecules ion both solution and the gas phase is well known and experimental and theoretical estimates of the binding energies of such complexes led us to believe that the attractive potential energy well would be amenable to investigation by low-energy scattering. We designed and constructed apparatus for measuring the elastic differential scattering cross-section at low incident ion energies. We find, however, that inelastic processes dominate the scattering.

Our apparatus (fig. 1) consists of an ion-gun assembly (I and L_1 in the figure) which can rotate ± 30° with respect to the stationary energy analysis section. Lithium ions from the thermal source (at I) are focussed into a flexible scattering chamber (c). The scattered ions are then focussed via lenses L_2 into a hemispherical electrostatic energy analyzer (A) which is capable of 2% FWHM energy resolution. The analyzed ions are then focussed by lenses L_3 into our Channeltron detector at D. The angular resolution is about 1.5° FWHM.

As a test of the capabilities of our apparatus we have performed some experiments with Li^+ ions of 10 eV incident ion energy incident upon neon as the target gas. An energy scan of the scattered Li^+ ions (fig. 2) typically has a FWHM of about 300 mV. This is consistent with the convolution of the thermal energy spread of the incident ions and the resolution of our analyzer. In addition, we can locate the maxima of these energy scans to within 15 or 20 mV. Thus we can compare the experimental and theoretical energy losses of the scattered ions due to momentum transfer to the target atom. The

theoretical and experimental scattered ion energies are plotted as a function of angle in fig. 3. We ascribe the 150 mV displacement, still within 2% of the theoretical values, to voltage calibration shifts due to contact potentials and sample gas effects. The differential scattering cross section (the lower curve in fig. 4) can be fitted with a 6-12 potential with a 0.13 eV well depth in accord with drift tube measurements. Thus we have found neon to be very useful in testing and calibrating our apparatus.

When we replace the neon with water vapor we find (fig. 5) that our energy scans are wider, with a FWHM of about a volt. The maxima in these scans are displaced by hundreds of millivolts from the expected location of the elastic peak (which would be quite close to the neon curve maximum in the figure) and there is no evidence of even a subsidiary elastic peak for the scattering from water. The displacement of the energy maximum as a function of angle is seen (in fig. 6) to be different in slope as well as magnitude from the corresponding quantity for the neon target experiments.

We thus conclude that an incident ion energies near 10 eV inelastic processes dominate the $Li^+ - H_2O$ scattering to the extent that the elastic processes cannot be distinguished. The structureless nature of the energy scans indicates to us that the closely-spaced rotational levels of the target molecules are involved, but we see no reason to rule out concurrent vibrational processes. Also note in fig. 6 that the difference between the <u>expected</u> location of the <u>elastic</u> peak in the energy scan and the actual location of the <u>inelastic</u> maximum increases as a function of angle, indicating that the degree of inelasticity may increase with decreasing impact parameter. (Note that for proper comparison the experimental points in fig. 6 should be translated up by about 0.1 eV in accordance with the calibration shift in fig. 3).

Figure 4 is a plot of a quantity with the rather confusing name of total differential cross section, that is, the cross section at any given laboratory angle summed over all observed processes at that angle.

Rotational inelasticities in low energy ion-molecule scattering have been noted previously. Giese and his co-workers [VIII ICPEAC (1973), p. 93] have found in the scattering of protons from a series of diatomic molecules that the rotational inelasticity increases with increasing dipole moments. This may mean that the long-range ion-dipole interaction facilitates rotational transitions during the collision process. To support this we took an energy scan of Li^+ scattered from N_2 and discovered no significant difference from the corresponding energy scan of Li^+ scattered from neon (see fig. 2).

We are extending the angular range and going to other incident ion energies for the $Li^+ - H_2O$ system and we will try other molecular targets and alkali-ion projectiles in the future.

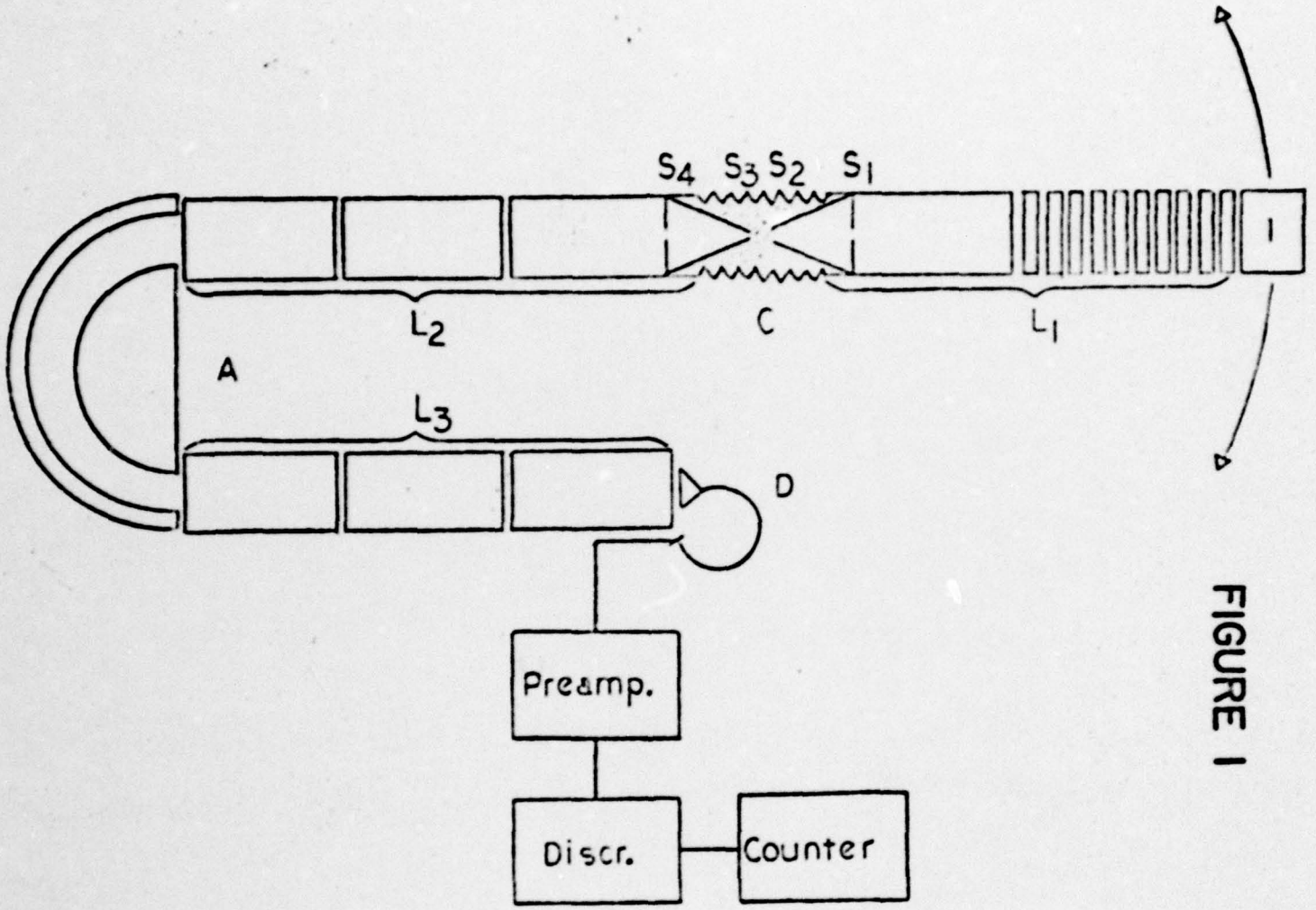

FIGURE 1

FIGURE 2

SCATTERED ION ENERGY
AT 9.5°

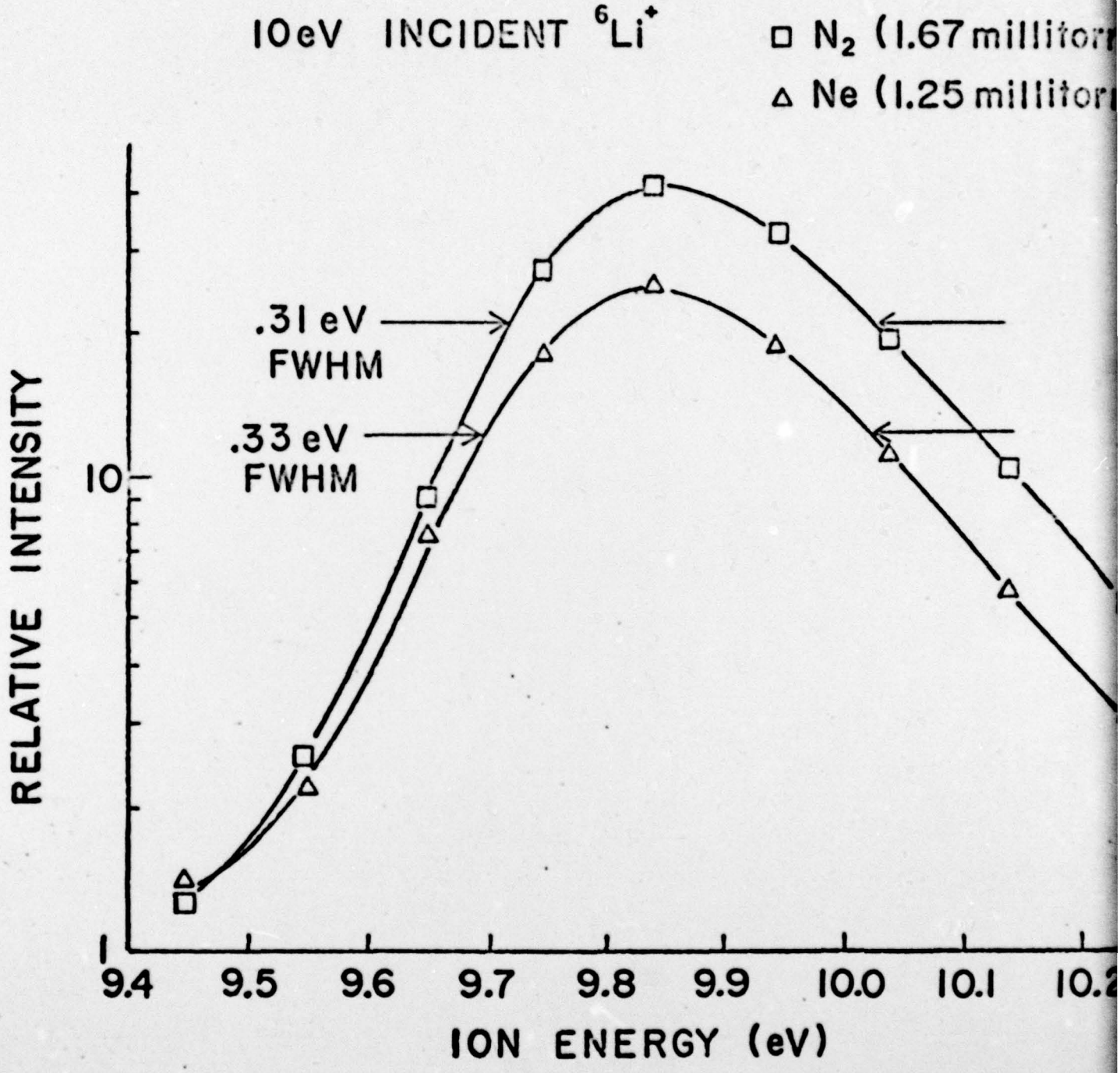

FIGURE 3

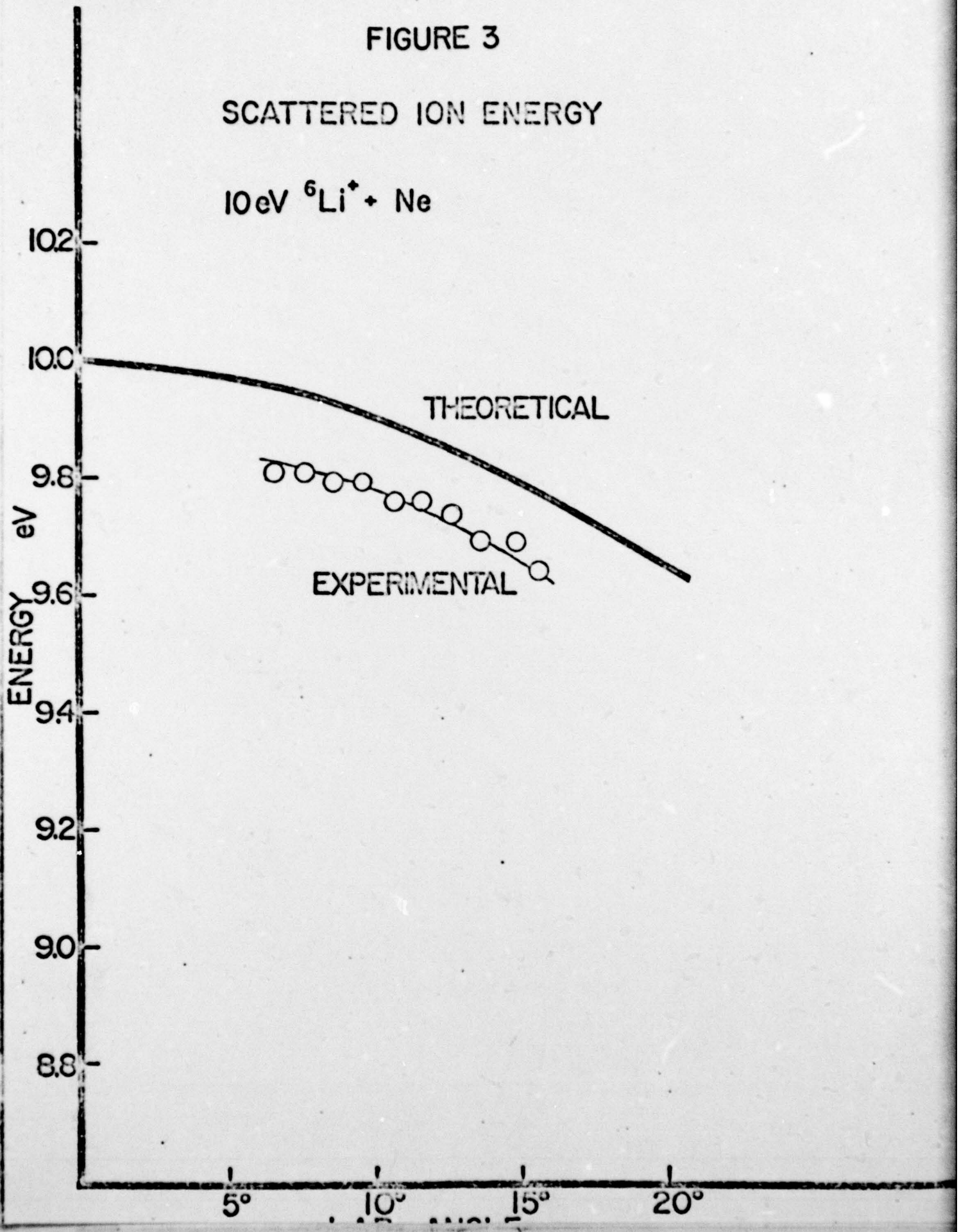
SCATTERED ION ENERGY
10 eV $^{6}Li^{+}$ + Ne
10.2
10.0
9.8
9.6
9.4
9.2
9.0
8.8
ENERGY eV
THEORETICAL
EXPERIMENTAL
5°
10°
15°
20°

FIGURE 4

RELATIVE DIFFERENTIAL CROSS SECTIONS AT 10eV INCIDENT ION ENERGY

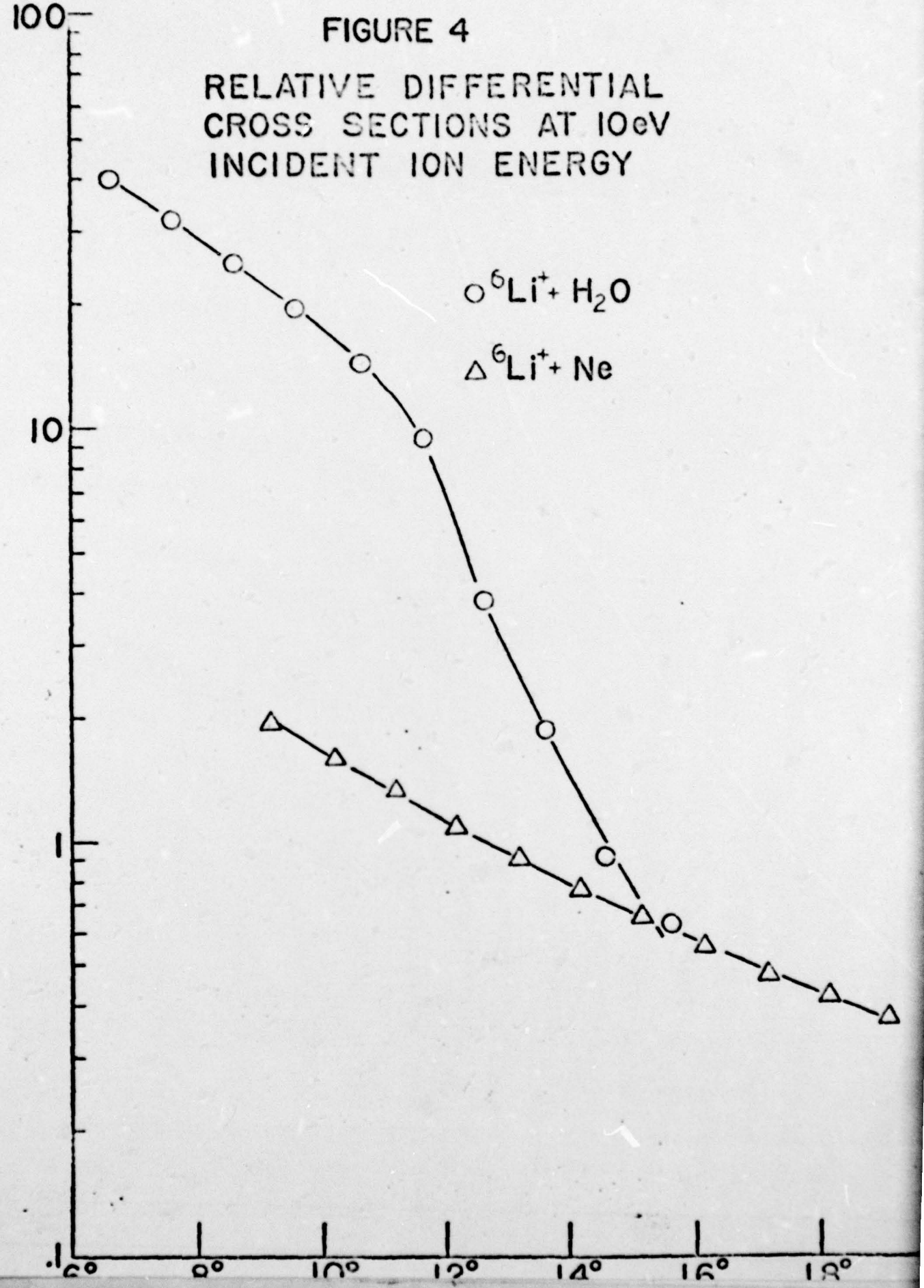

FIGURE 5

SCATTERED ION ENERGY
AT 10.6°

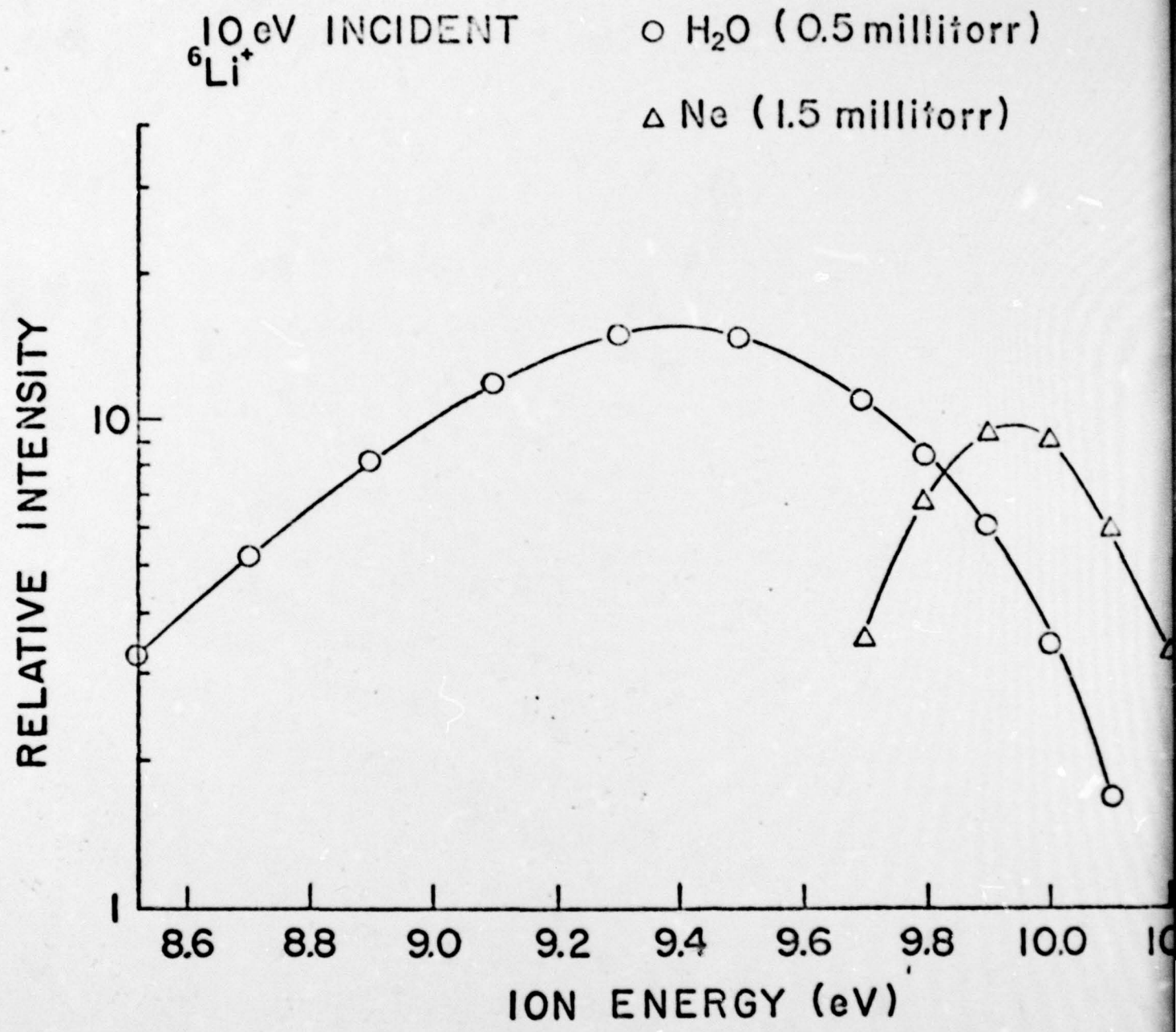

FIGURE 6

SCATTERED ION ENERGY

10 eV $^{6}Li^{+} + H_2O$